14 Transducers

Information technology requires technology, and it requires information. From the earliest computers (and people), external interfaces have been essential to their intelligence [Turing, 1950]. *Sensors* are used to convert a parameter of interest to a from that is more convenient to use. The most familiar sensors provide an electrical output, but many other kinds of mappings are possible. An optical sensor that modulates light in a fiber might be appropriate if interference, explosion, or speed is a concern. Sensors are sometimes called *transducers*, although transduction is more correctly used to refer to bidirectional mechanisms such as piezoelectricity that can convert between pressure and charge. There are almost as many sensors as sensees. The enormous diversity of things that can be measured, and of people doing the measuring, is reflected in the range of available solutions. Because many of these mechanisms are complex, with embodiments that are considered to be trade secrets, and the safety of nuclear reactors or rocketships depends on them, the literature is a curious combination of profound insights and received wisdom that is repeated for reasons of liability rather than scientific merit. There is certainly a lot of room left for innovation.

We've already covered many important types of sensors. The purpose of this chapter is not to fill in the remaining ones – that would fill a shelf full of books. It is to introduce some of the physics that follows from relaxing assumptions we've been relying on, and show the applications to sensing that then follow. The first section will drop the independence of particle states used in deriving partition functions, which will lead to superconductivity and magnetic field sensors that can resolve individual flux quanta. Then comes eliminating the assumption that thermodynamic distributions are in equilibrium. Instead of just using a p-n junction as a thermometer by measuring the reverse-biased current, we'll see that because it is not in thermal equilibrium the presence of an electrical current through it lets it also act as a refrigerator. Finally, we'll question whether space and time themselves are independent or dependent variables, and find the relativistic corrections needed to make GPS work.

14.1 MANY-BODY EFFECTS

Because most devices operate somewhere above absolute zero, we've relied on statistical mechanics to find the occupancy of their available particle states. This has proceeded by finding the states for a single particle, and then maximizing the entropy of the distribution over those states subject to appropriate constraints. While a widely applicable

approach, this ignores the possibility that the multi-particle states are very different from those available to single particles. The consequences of these much more challenging calculations are called variously *many-body*, *cooperative*, or *collective* effects. We'll see next that electrons in a metal provide a striking example of such behavior.

14.1.1 Superconductivity

In Chapter 11 electrons in a metal were found to be well described by nearly-free plane-wave states, occupied up to a Fermi energy E_F. The negatively-charged electrons travel in a sea of positive ionic charge. A reasonable, and quite incorrect, assumption is that the electrons weakly repel each other. What actually happens is that the conduction electrons zipping along at the Fermi energy quickly pass the much heavier positive ions. An ion is attracted towards a passing electron, but by the time the ion begins moving the electron is long since gone. A second electron that passes by will be attracted by the positive wake left by the first electron, effectively being drawn towards the electron. What's actually happening is that the second electron is absorbing a lattice phonon excited by the first one.

To find the possible states of the two-electron system, let's look at those that have opposite momentum so that the combined system is at rest

$$\psi = \sum_k a_k e^{i\vec{k}\cdot\vec{x}_1} e^{-i\vec{k}\cdot\vec{x}_2} = \sum_k a_k e^{i\vec{k}\cdot(\vec{x}_1-\vec{x}_2)} \quad . \tag{14.1}$$

This must satisfy the two-electron Schrödinger equation

$$-\frac{\hbar^2}{2m}\left(\nabla_1^2 + \nabla_2^2\right)\psi + V\left(\vec{x}_1, \vec{x}_2\right)\psi = E\psi \quad , \tag{14.2}$$

where V is their effective interaction potential. Plugging in the wave function, multiplying both sides by $e^{i\vec{k}'\cdot(\vec{x}_1-\vec{x}_2)}$, and then integrating over all space and using the orthonormality of the eigenstates gives

$$\left(E - 2\epsilon_k\right) a_k = \sum_{k'} V_{kk'} a_{k'} \quad , \tag{14.3}$$

where ϵ_k are the single-particle eigenstate energies, and $V_{kk'}$ is the expectation value of the interaction potential between a pair of momentum states.

Because of Pauli exclusion with all of the core electrons, a_k will vanish for k below the Fermi level k_F (Chapter 11). And $V_{kk'}$ will be small above some cutoff $k > k_c$, because if an electron passes by an ion too quickly the ion won't move. A Nobel-prize-worthy approximation is to assume that the potential is zero below the Fermi energy E_F and also above a cutoff $E_F + E_c(k_c)$, and has a constant value $-V$ in between [Cooper, 1956]. Then the potential comes out of the sum

$$a_k = -V \frac{\sum_{k=k_F}^{k_c} a_{k'}}{E - 2\epsilon_k} \quad , \tag{14.4}$$

which can be simplified by summing both sides over k:

$$\frac{1}{V} = \sum_{k=k_F}^{k_c} \frac{1}{2\epsilon_k - E} \quad . \tag{14.5}$$

Because of the large number of states, the sum can be replaced by an integral weighted by the density of states N_F at the Fermi energy

$$\begin{aligned}\frac{1}{V} &= N_\mathrm{F}\int_{E_\mathrm{F}}^{E_\mathrm{F}+E_\mathrm{c}} \frac{1}{2\epsilon - E}\, d\epsilon \\ &= \frac{N_\mathrm{F}}{2}\log\left(\frac{2E_\mathrm{F}+2E_\mathrm{c}-E}{2E_\mathrm{F}-E}\right) \\ E\left(1-e^{-2/N_\mathrm{F}V}\right) &= 2E_\mathrm{F}\left(1-e^{-2/N_\mathrm{F}V}\right) - 2E_\mathrm{c}e^{-2/N_\mathrm{F}V} \\ E &\approx 2E_\mathrm{F} - 2E_\mathrm{c}e^{-2/N_\mathrm{F}V} \quad . \end{aligned} \tag{14.6}$$

This is a remarkable result: for any value of V, no matter how small, it is energetically favorable for the electrons to form bound pairs. These are called *Cooper pairs* in honor of Leon Cooper, who first did this calculation. At high temperatures thermal energies exceed the binding energy, but as a metal is cooled it becomes significant.

Even more remarkable is the symmetry implication. Because electrons are fermions their wave functions must be antisymmetric. But because a Cooper pair has two electrons, interchanging a pair of electrons changes the sign twice, leaving it unchanged. This means that Cooper pairs are bosons. And that means that an arbitrary number can be in the same state, and in particular they can all be in the ground state. When this happens to bosons it is called *Bose–Einstein condensation*, and it can even occur with entire atoms [Anderson *et al*., 1995]. When it happens to Cooper pairs the result is *superconductivity*.

Superconductivity is explained by the *BCS theory*, named for its developers John Bardeen and Robert Schrieffer along with Leon Cooper [Bardeen *et al*., 1957]. The difficulty in working out the details of the Bose–Einstein condensation of Cooper pairs is that each electron must wear two hats: it must be a member of a pair to act as a boson, and it must also act as a fermion to provide the exclusion that makes pairing possible. The resulting symmetry explains why superconductors carry *persistent currents* without loss. In a normal metal, resistance occurs through electrons losing energy in inelastic collisions to phonons. But in a superconductor, each electron is part of a collective state that reflects not just its pairing but also its contribution through exclusion to many other pairs. For one of these electrons to scatter it must destroy the symmetry of this much larger state, an enormously unfavorable event that happens exceedingly rarely.

Since the pairs are locally all in the same state, a collective wave function $\psi(\vec{x},t) = \sqrt{n}\, e^{i\varphi}$ can be defined, where $|\psi|^2 = n$ is the pair density and φ is their phase. Ginzberg and Landau originally assumed this relationship [Ginzburg & Landau, 1950], and it was later justified as an approximation to the full BCS theory when the density and phase vary slowly compared to the pair size. In terms of ψ, the current associated with the pairs can be found from the expectation value for their velocity $\vec{v}$ times their charge $2e$

$$\vec{J} = \int \psi^* 2e\vec{v}\psi \; d\vec{x} \quad . \tag{14.7}$$

In the CGS units usually used for superconductivity, the momentum of a particle in an electromagnetic field has an extra piece

$$\vec{p} = m\vec{v} + q\vec{A}/c \tag{14.8}$$

due to the force associated with moving through the vector potential $\vec{A}$ [Goldstein, 1980],

therefore plugging in the momentum operator shows that the velocity is found from

$$\vec{v} = -i\frac{\hbar}{m}\nabla - \frac{q}{mc}\vec{A} \quad . \tag{14.9}$$

The current is then

$$\begin{aligned}\vec{J} &= \int \psi^* 2e\vec{v}\psi \, d\vec{x} \\ &= \int \sqrt{n}\ \exp(-i\varphi) 2e \left(-i\frac{\hbar}{m}\nabla - \frac{2e}{mc}\vec{A}\right) \sqrt{n}\ \exp(i\varphi)\, d\vec{x} \\ &= \frac{2ne}{m}\left(\hbar\nabla\varphi - \frac{2e}{c}\vec{A}\right) \quad . \end{aligned} \tag{14.10}$$

Taking the curl provides a relationship between $\vec{J}$ and $\vec{B}$

$$\nabla \times \vec{J} = -\frac{4ne^2}{mc}\nabla \times \vec{A} = -\frac{4ne^2}{mc}\vec{B} \tag{14.11}$$

called the *London equation*. Since $\nabla \times \vec{B} = (4\pi/c)\vec{J}$,

$$\begin{aligned}\nabla \times \nabla \times \vec{B} &= \frac{4\pi}{c}\nabla \times \vec{J} \\ -\nabla^2 \vec{B} &= -\frac{4\pi}{c}\frac{4ne^2}{mc}\vec{B} \quad . \end{aligned} \tag{14.12}$$

This differential equation shows that the magnetic field is exponentially screened at the surface, and hence that the supercurrent travels within the *London penetration depth* to cancel the field in the interior. This is the origin of the *Meissner effect* introduced in Chapter 13: superconductors expel magnetic fields.

Consider now a superconducting loop threaded by a flux Φ. In the interior where there are no currents, equation (14.10) becomes $\hbar c\nabla\varphi = 2e\vec{A}$. Integrating this around the loop,

$$\begin{aligned}\hbar c\nabla\varphi &= 2e\vec{A} \\ \hbar c \oint \nabla\varphi \cdot d\vec{l} &= 2e \oint \vec{A} \cdot d\vec{l} \\ \hbar c\Delta\varphi &= 2e \int \nabla \times \vec{A} \cdot d\vec{A} \\ &= 2e \int \vec{B} \cdot d\vec{A} \\ &= 2e\Phi \\ \Delta\varphi &= \frac{2e}{\hbar c}\Phi \quad . \end{aligned} \tag{14.13}$$

But

$$\Delta\varphi = 2\pi m \tag{14.14}$$

must hold, where m is an integer, so that the phase is continuous around the loop. This means that the supercurrent in the loop varies as a function of the external field to enforce a *flux quantization* condition

$$\Phi = \frac{2\pi\hbar c}{2e}m = \frac{hc}{2e}m \equiv \Phi_0 m \quad . \tag{14.15}$$

14.1.2 Junctions and Interferometers

As with semiconductors, superconducting devices rely on junctions. Consider two superconductors separated by an insulating layer so thin that Cooper pairs can tunnel through it. This geometry is called a *Josephson junction*, after Brian Josephson who as a graduate student predicted its unexpected behavior [Josephson, 1962].

Let ψ_1 and ψ_2 be the wave functions on either side of the junction, and r be the characteristic rate for tunneling. Then the rate of change of the wave functions due to tunneling is found from the time-dependent Schrödinger equation

$$i\hbar\frac{\partial\psi_1}{\partial t} = \hbar r\psi_2 \quad i\hbar\frac{\partial\psi_2}{\partial t} = \hbar r\psi_1 \quad . \tag{14.16}$$

Substituting $\psi_1 = \sqrt{n_1}\ \exp(i\varphi_1)$ and $\psi_2 = \sqrt{n_2}\ \exp(i\varphi_2)$ shows that

$$i\hbar\frac{1}{2\sqrt{n_1}}\frac{\partial n_1}{\partial t}\exp(i\varphi_1) + i\hbar\sqrt{n_1}\ \exp(i\varphi_1)\, i\frac{\partial\varphi_1}{\partial t} = \hbar r\sqrt{n_2}\ \exp(i\varphi_2)$$

$$\frac{\partial n_1}{\partial t} + 2in_1\frac{\partial\varphi_1}{\partial t} = -2ir\sqrt{n_1 n_2}\ \exp[i(\varphi_2-\varphi_1)] \quad , \tag{14.17}$$

which has a real part

$$\frac{\partial n_1}{\partial t} = 2r\sqrt{n_1 n_2}\ \sin(\varphi_2-\varphi_1) \quad . \tag{14.18}$$

The current density J across the junction is proportional to the rate of change of the pair density. If the superconductors are identical then $n_1 \approx n_2$, so combining all the constants into a coefficient J_0 gives

$$J = J_0\sin(\varphi_2-\varphi_1) \quad . \tag{14.19}$$

This is quite unlike anything we've seen before: there is a current in the absence of an applied voltage, with a sinusoidal dependence on the quantum phase difference. This is called the *DC Josephson effect*.

Now turn on a potential V across the junction, adding an energy term to the Hamiltonian from the pair charge $-2e$

$$i\hbar\frac{\partial\psi_1}{\partial t} = \hbar r\psi_2 - eV\psi_1 \quad i\hbar\frac{\partial\psi_2}{\partial t} = \hbar r\psi_1 + eV\psi_2 \quad . \tag{14.20}$$

Once again plugging in the wave functions on each side,

$$\frac{\partial n_1}{\partial t} + 2in_1\frac{\partial\varphi_1}{\partial t} = -2ir\sqrt{n_1 n_2}\ \exp[i(\varphi_2-\varphi_1)] + i\frac{2eV}{\hbar}n_1 \quad , \tag{14.21}$$

which has an imaginary part

$$\frac{\partial\varphi_1}{\partial t} = -r\sqrt{\frac{n_2}{n_1}}\cos(\varphi_2-\varphi_1) + \frac{eV}{\hbar} \quad . \tag{14.22}$$

Taking $n_1 \approx n_2$ and subtracting the corresponding equation for $\partial\varphi_2/\partial t$ leaves

$$\frac{\partial(\varphi_2-\varphi_1)}{\partial t} = -\frac{2eV}{\hbar} \quad . \tag{14.23}$$

The current density through the junction is found by integrating this and plugging it into the real part of equation (14.21):

$$J = J_0 \sin\left(-\frac{2eV}{\hbar}t\right) \quad . \tag{14.24}$$

Now the current oscillates, with the proportionality between frequency and voltage given by the ratio of fundamental constants $e/\hbar$. This is the *AC Josephson effect*.

The same thing works in reverse: if a Josephson junction is irradiated with microwaves it induces a supercurrent with DC steps in the I-V curve at voltages

$$V = n\frac{h}{2e}f \tag{14.25}$$

for integer n [Shapiro, 1963]. This *inverse AC Josephson effect* converts frequency to voltage based on just fundamental constants, and hence can be used as a voltage reference [Hamilton, 2000]. Given the small size of the steps (2.067 μV/GHz) hundreds of thousands of junctions are required to add up to volts [Burroughs *et al*., 2011].

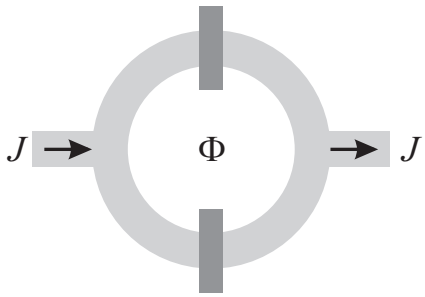

Figure 14.1. A SQUID. Current flows through two thin insulating barriers in a superconducting loop.

Finally, connect two Josephson junctions in a loop to from a *Superconducting Quantum Interference Device* (*SQUID*), as shown in Figure 14.1. From equation (14.13) the phase difference around the loop must be $2e\Phi/\hbar c$, and from equation (14.19) the total current is the sum over the two branches, each of which goes as the sine of the phase difference over the junctions, so the combined current is

$$\begin{aligned} J &= J_0\left[\sin\left(\varphi_0 + \frac{e}{\hbar c}\Phi\right) + \sin\left(\varphi_0 - \frac{e}{\hbar c}\Phi\right)\right] \\ &= 2J_0 \sin(\varphi_0)\cos\left(\frac{e\Phi}{\hbar c}\right) \quad , \end{aligned} \tag{14.26}$$

where φ_0 is an overall phase. Because of the interference between the two branches the current is a periodic function of the flux, which is why this geometry is called an interferometer. What makes it so interesting is the size of the period. A single *flux quantum* is just

$$\Phi_0 = \frac{2\pi\hbar c}{2e} = \frac{hc}{2e} = 2.07\times10^{-7}\ \mathrm{G}\cdot\mathrm{cm}^2 \quad . \tag{14.27}$$

Measuring the current oscillations in a SQUID is not only the most sensitive way to detect magnetic fields, it can also be used to determine many other small quantities (such

as voltage) by converting them to a magnetic field first (with a current loop for measuring picovolts [Eriksson *et al*., 1999]).

Finally, coupled Josephson junctions can do logic with the quantized flux. One attraction is the speed; *Rapid Single Flux Quantum* (*RSFQ*) circuits can operate with picosecond clocks [Mukhanov *et al*., 1987]. And another is power; *Adiabatic Quantum Flux Parametron* (*AQFP*) devies use an AC rather than DC bias for zeptojoule bit energies [Takeuchi *et al*., 2013].

14.2 NON-EQUILIBRIUM THERMODYNAMICS

Many-body effects can profoundly change the states available to a system, as we saw in superconductivity, but these states are still populated in equilibrium with the maximum-entropy distribution (Section 3.4). Here we'll relax the assumption of thermal equilibrium, and find still more surprises in the behavior of electrons in a metal.

The entropy S is an *extensive* quantity that is a function of the size of a system, unlike *intensive* properties like temperature that have the same value in subsystems. It will in turn depend on other extensive variables, such as the total energy and number of particles, with densities $f_1, f_2, \ldots$. Using the chain rule, the rate of change of the entropy is

$$\begin{aligned} \frac{\partial S}{\partial t} &= \sum_i \frac{\partial S}{\partial f_i}\frac{\partial f_i}{\partial t} \\ &\equiv \sum_i F_i \frac{\partial f_i}{\partial t} \quad . \end{aligned} \tag{14.28}$$

This defines intensive thermodynamic forces F_i conjugate to the f_i's, which will vanish at the peak of the entropy. If there is a current density $\vec{J}_i$ transporting the quantity f_i (such as the local number of electrons), it will likewise lead to an entropy current

$$\vec{J}_S = \sum_i F_i \vec{J}_i \quad . \tag{14.29}$$

If f_i is conserved, then by Gauss' Theorem the local rate of change will be due to the divergence of the current

$$0 = \frac{\partial f_i}{\partial t} + \nabla \cdot \vec{J}_i \quad . \tag{14.30}$$

Because entropy can be created and destroyed, its rate of change is

$$\begin{aligned} \frac{dS}{dt} &= \frac{\partial S}{\partial t} + \nabla \cdot \vec{J}_s \\ &= \sum_i F_i \frac{\partial f_i}{\partial t} + \nabla \cdot \sum_i F_i \vec{J}_i \\ &= \sum_i F_i \frac{\partial f_i}{\partial t} + \sum_i \vec{J}_i \cdot \nabla F_i + \sum_i F_i \underbrace{\nabla \cdot \vec{J}_i}_{-\frac{\partial f_i}{\partial t}} \end{aligned}$$

$$= \sum_i \vec{J}_i \cdot \nabla F_i \quad . \tag{14.31}$$

Since $TdS = dQ$, the left hand side represents dissipation. The right hand side is the product of currents and forces that drive them; think of $P = IV$. It is experimentally found in many systems near equilibrium that these currents and forces are related linearly,

$$\vec{J}_i = \sum_j L_{ij} \nabla F_j \quad , \tag{14.32}$$

such as Ohm's Law for electrical conduction or Fourier's Law for thermal conduction. This equation says that the current moves in the direction that maximizes the entropy, with a flux proportional to the gradient, defining *linear non-equilibrium thermodynamics*.

The microscopic laws in a system put important constraints on the macroscopic L_{ij} coefficients. To see this, remember that

$$p(S) = \frac{e^{S/k_B}}{\int e^{S/k_B}} \tag{14.33}$$

(equation 3.46). Therefore the product of one of the extensive variables f_i and a thermodynamic force F_j is

$$\begin{aligned}
\langle f_i F_j \rangle &= \int f_i F_j p(\vec{f})\, d\vec{f} \\
&= \int f_i \frac{\partial S}{\partial f_j} p(\vec{f})\, d\vec{f} \\
&= \frac{\int f_i \frac{\partial S}{\partial f_j} e^{S(\vec{f})/k_B}\, d\vec{f}}{\int e^{S(\vec{f})/k_B}\, d\vec{f}} \\
&= k_B \frac{\int f_i \frac{\partial}{\partial f_j} e^{S(\vec{f})/k_B}\, d\vec{f}}{\int e^{S(\vec{f})/k_B}\, d\vec{f}} \\
&= -k_B \frac{\int \frac{\partial f_i}{\partial f_j} e^{S(\vec{f})/k_B}\, d\vec{f}}{\int e^{S(\vec{f})/k_B}\, d\vec{f}} \quad \text{(integrate by parts)} \\
&= -k_B \delta_{ij} \quad .
\end{aligned} \tag{14.34}$$

For convenience, choose units for f and F that vanish in equilibrium. Then their deviation from equilibrium will relax with the same linear coefficients

$$\frac{df_i}{dt} = \sum_j L_{ij} F_j \quad . \tag{14.35}$$

This is an experimentally-justified conjecture first made by [Onsager, 1931]. It implies that

$$\left\langle f_i \frac{df_j}{dt} \right\rangle = \sum_k L_{jk} \langle f_i F_k \rangle$$

$$= -k_B L_{ji} \tag{14.36}$$

and

$$\left\langle \frac{df_i}{dt} f_j \right\rangle = \sum_k L_{ik} \langle F_k F_j \rangle$$
$$= -k_B L_{ij} \quad . \tag{14.37}$$

The time derivatives are defined as the expectations of the change over an interval τ that is long compared to the time scale of microscopic dynamics but short compared to the time scale for macroscopic changes,

$$\left\langle f_i \frac{df_j}{dt} \right\rangle = \frac{1}{\tau} \left\langle f_i(t) \left[f_j(t+\tau) - f_j(t) \right] \right\rangle$$
$$= \frac{1}{\tau} \langle f_i(t) f_j(t+\tau) \rangle - \frac{1}{\tau} \langle f_i(t) f_j(t) \rangle \tag{14.38}$$

and

$$\left\langle \frac{df_i}{dt} f_j \right\rangle = \frac{1}{\tau} \langle [f_i(t+\tau) - f_i(t)] f_j(t) \rangle$$
$$= \frac{1}{\tau} \langle f_i(t) f_j(t+\tau) \rangle - \frac{1}{\tau} \langle f_i(t) f_j(t) \rangle \quad . \tag{14.39}$$

But most physical laws, other than magnetism, are unchanged if $t \to -t$, therefore

$$\langle f_i(t) f_j(t+\tau) \rangle = \langle f_i(-t) f_j(-t-\tau) \rangle$$
$$= \langle f_i(t+\tau) f_j(t) \rangle \quad . \tag{14.40}$$

This requires that

$$\left\langle \frac{df_i}{dt} f_j \right\rangle = \left\langle f_i \frac{df_j}{dt} \right\rangle \tag{14.41}$$

and hence

$$L_{ij} = L_{ji} \quad . \tag{14.42}$$

This is *Onsager's Reciprocity Theorem*. It provides a direct connection between apparently unrelated phenomena, as we'll see in the next section. If there are magnetic fields present, then B must be replaced with $-B$ along with changing the sign of t.

14.2.1 Thermoelectricity

Now let's apply this theory to electrons in a metal. Their energy U will vary with changes in both the entropy dS and the particle number dN

$$dU = TdS + (\mu + qV)dN \tag{14.43}$$

through the chemical potential μ (equation 11.5) and the electrical potential V. The sum $\mu + qV$ is called the *electrochemical potential*.

The entropy change is thus

$$dS = \frac{1}{T} dU - \frac{\mu + qV}{T} dN \quad , \tag{14.44}$$

and the currents are

$$\vec{J}_S = \frac{1}{T}\vec{J}_U - \frac{\mu + qV}{T}\vec{J}_N \quad , \tag{14.45}$$

or since $TdS = dQ$ the heat current J_Q is

$$\vec{J}_Q = \vec{J}_U - (\mu + qV)\vec{J}_N \quad . \tag{14.46}$$

Therefore from equation (14.31) the derivative of the entropy is

$$\begin{aligned}\frac{dS}{dt} &= \vec{J}_U \cdot \nabla\left(\frac{1}{T}\right) - \vec{J}_N \cdot \nabla\left(\frac{\mu + qV}{T}\right) \\ &= \vec{J}_U \cdot \nabla\left(\frac{1}{T}\right) - (\mu + qV)\vec{J}_N \cdot \nabla\left(\frac{1}{T}\right) - \frac{1}{T}\vec{J}_N \cdot \nabla(\mu + qV) \\ &= \underbrace{\left[\vec{J}_U - (\mu + qV)\vec{J}_N\right]}_{\vec{J}_Q} \cdot \nabla\left(\frac{1}{T}\right) - \vec{J}_N \cdot \frac{1}{T}\nabla(\mu + qV) \quad .\end{aligned} \tag{14.47}$$

Near equilibrium, these pairs of conjugate currents and forces will be related by linear coefficients

$$\begin{aligned}\vec{J}_Q &= L_{QQ}\nabla\left(\frac{1}{T}\right) - L_{QN}\frac{1}{T}\nabla(\mu + qV) \\ \vec{J}_N &= L_{NQ}\nabla\left(\frac{1}{T}\right) - L_{NN}\frac{1}{T}\nabla(\mu + qV) \quad .\end{aligned} \tag{14.48}$$

The first represents the thermal current, and the second is the electrical current.

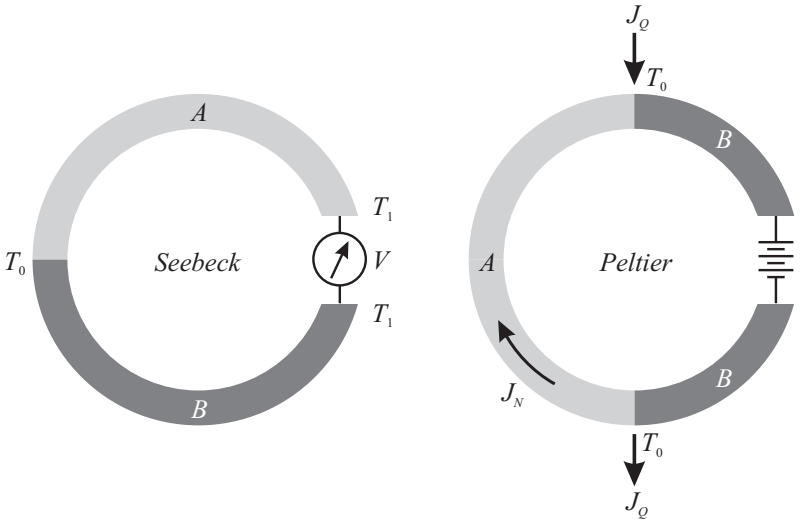

Figure 14.2. Thermoelectric effects.

Crucially, these coefficients are material-dependent. Consider the two cases in Figure 14.2. In the first, two materials A and B meet at a junction at a temperature T_0, and

are connected to a voltmeter at a temperature T_1. Since the voltmeter draws no electrical current, $J_N = 0$, so from equation (14.48)

$$\begin{aligned} 0 &= L_{NQ}\nabla\left(\frac{1}{T}\right) - L_{NN}\frac{1}{T}\nabla(\mu + qV) \\ -\nabla(\mu + qV) &= -\frac{TL_{NQ}}{L_{NN}}\,\nabla\left(\frac{1}{T}\right) \\ &= \frac{L_{NQ}}{TL_{NN}}\,\nabla T \\ &\equiv S\nabla T \quad . \end{aligned} \tag{14.49}$$

The gradient of the electrochemical potential is equal to the thermal gradient times the *thermopower* or *Seebeck coefficient* S. Integrating the thermal gradient along A and B will give the same result $T_1 - T_0$, but integrating the electrochemical gradient will give a different answer because the materials are different. This is called the *Seebeck effect*, and is used in *thermocouples* to measure temperature. There are many standard thermocouple pairs with known dependence of S on T. For example, a junction between copper and constantan (an alloy of 55% Cu with 45% Ni), called a *type T* thermocouple, produces 40.9 μV/°C at 25 °C.

There is one subtlety in the use of a thermocouple: there will be extra unintentional thermocouple junctions at the contacts between the leads and the voltmeter. Eliminating their influence requires either fixing their temperature (historically, with an ice bath) or measuring it (typically with a temperature-dependent resistor or diode, Chapter 11). While it might appear to be nonsensical to use a thermometer in order to make a thermometer work, among the many desirable features of thermocouples that lead to their routine use are their low cost, small size, and wide temperature range. These are all consequences of the fact that the sensor is just a junction between dissimilar metals. For many applications these benefits more than justify the addition of an extra electronic thermometer that does not need compensation at the instrument connections.

The second circuit in Figure 14.2 drives an electrical current around a loop between the two materials, which are held at the same temperature. Now $\nabla(1/T) = 0$, so the ratio of the currents is

$$\frac{J_Q}{J_N} \equiv \Pi = \frac{L_{QN}}{L_{NN}} \tag{14.50}$$

This defines the *Peltier coefficient* Π. To maintain the isothermal condition, a thermal current must flow into one junction and out of the other one if there is an electrical current. That means that the circuit acts as a heat pump, generating heat on one side and removing it on the other. Unlike ordinary ohmic heating this process is reversible, and unlike ohmic heating it can also be used to cool things.

Because the Onsager relations require that $L_{QN} = L_{NQ}$,

$$\Pi = ST \quad . \tag{14.51}$$

There's no *a priori* reason to expect a relationship between the coefficients in circuits acting as a thermometer and a refrigerator; it is a consequence of the time-reversal invariance of their governing equations.

Materials for practical *Peltier coolers* require a large thermopower, along with a high

electrical conductivity σ and low thermal conductivity κ. These can be combined to define a dimensionless figure of merit

$$ZT \equiv \frac{S^2\sigma}{\kappa} \quad . \tag{14.52}$$

The most common choice is doped semiconducting bismuth telluride, which has $ZT \sim 1$.

The junctions in a Peltier cooler are wired in series to increase the device resistance in order to reduce the ohmic heating losses, and they can be stacked in parallel to increase the temperature drop. They find application in cooling without moving parts everything from chips to submarines. One of the most important applications is cooling other sensors, such as infrared detectors, which have sensitivities that improve with decreasing temperature. The maximum temperature difference that can be achieved is set by the decrease of the thermopower at low tempeatures as the electron scattering rate that establishes the thermalization decreases. A temperature difference of about 100 °C is the limit for bismuth telluride with no heat load, with a maximum efficiency ratio of heat pumped to power supplied of ∼0.25–0.5 due to internal losses.

14.2.2 Piezoelectricity

A second important example of a reciprocity relationship is between force and electric fields, called *piezoelectricity*. If an electric field $\vec{E}$ and a stress (force per area) $\vec{T}$ are applied to a material, the resulting polarization $\vec{P}$ is

$$\vec{P} = \mathbf{d}\vec{T} + \chi\vec{E} \quad , \tag{14.53}$$

where χ is the susceptibility matrix and $\mathbf{d}$ is the *piezoelectric* matrix. The corresponding strain $\vec{S}$ (relative displacement) is

$$\vec{S} = \mathbf{c}\vec{T} + \mathbf{d}\vec{E} \quad , \tag{14.54}$$

where $\mathbf{c}$ is the mechanical *compliance* matrix. Because of Onsager's Theorem the $\mathbf{d}$'s are the same. Once again, there's no *a priori* reason to expect the electrical field produced in response to a mechanical force to have the same coefficient as the displacement produced by a field.

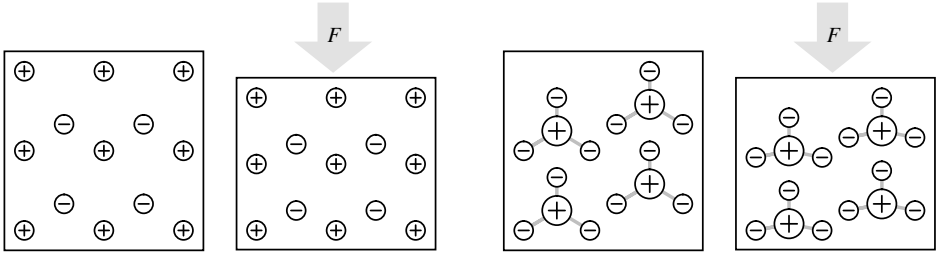

Figure 14.3. Charge locations in the unit cell for ferroelectric (left) and non-ferroelectric (right) piezoelectric materials.

There are two kinds of piezoelectricity, shown in Figure 14.3. In a *ferroelectric* material there is a dipole moment that is intrinsic to the unit cell because of offset interpenetrating

lattices. The moment will change its value if the aspect ratio of the unit cell changes. In non-ferroelectric piezoelectricity there is no intrinsic moment, but an applied force can break the symmetry of the local charge distribution and induce one. Ferroelectrics are always piezoelectric, but the converse is not true. Barium titanate ($BaTiO_3$) is an example of the former; quartz the latter. Even bones are piezoelectric, which is how they grow to best resist stress [Fukada & Yasuda, 1957].

Because of the reciprocity relationship, piezoelectrics are equally useful as acoustic detectors and generators. If electrodes are deposited on the top and bottom of a piezoelectric, a mechanically-induced change in the polarization will induce charge in the electrodes, and *vice versa*. Since the material is a charge source rather than a voltage source the response falls off at low frequencies, and piezoelectrics need to be used with high input-impedance instrumentation to not load them.

If the relative charge positions can change in the unit cell, ferroelectrics will have $\vec{E}, \vec{P}$ curves analogous to the $\vec{H}, \vec{M}$ curves of a ferromagnet (hence the name), and a Curie temperature above which their ordering is lost. The hysteresis can be applied in electrically-addressed non-volatile memories [Scott, 1998] and displays [Surguy, 1993].

Ferroelectric piezoelectrics are *poled* by heating the material under an applied field to induce the polarization, possibly along with a mechanical stress to align crystalline domains. The anisotropic piezoelectric axes are conventionally defined so that "3" points in the direction of the thickness, "1" points in the extrusion direction, and "2" is transverse. The d_{33} coefficient corresponds to a force applied across the thickness inducing a field in that direction. The common ceramic piezoelectric PZT ($Pb(Zr,Ti)O_3$) has a d_{33} of $\sim$280 pC/N. The polymer PVDF (polyvinylidene fluoride) has a d_{33} of -33 pC/N. While this is smaller than that of PZT, PVDF is attractive because it is thin, flexible, and broadband [Kawai, 1969]. The d_{31} coefficient, which represents a transverse field being produced by in-plane stress, is typically an order of magnitude smaller, but is very useful because the mechanical response can be much greater.

14.3 RELATIVITY

The last assumption to relax is that time and space are independent of the observer. While that might sound more like a matter for philosophy or science fiction than engineering design, relativistic effects have significant implications for applications such as navigation that rely on accurate time-keeping. To make that connection we'll need to first look at how time is measured, then how relativity corrects it, and finally at position measurement.

14.3.1 Clocks

The reciprocal relationship between polarization and displacement in a piezoelectric material means that its electrical behavior depends on its mechanical properties. Figure 14.4 shows the effective circuit for a piezoelectric crystal between electrodes. In parallel with the electrical capacitance C_e, there is a series RLC circuit associated with its mechanical response. The capacitance C_m represents energy storage in physical displacements, the inductance L_m comes from the inertial mass of the material, and the resistance R_m is due

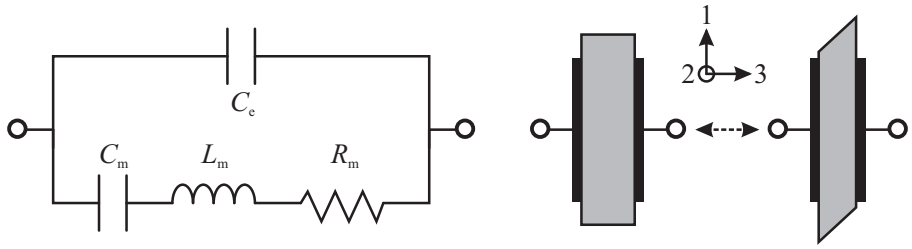

Figure 14.4. The effective circuit for a piezoelectric resonator, and the thickness shear mode.

to its mechanical dissipation. Because of the piezoelectricity, these all appear as electrical components connected to the electrodes.

Now consider what happens when this circuit is connected in the feedback network of an amplifier. If an amplifier's output is related to its input by inverting gain $y = -Ax$, and if the feedback circuit scales the output by a complex coefficient $x = F(\omega)y$, then $x = -AF(\omega)x$. This is only possible if $AF(\omega) = -1$, therefore the phase of F must be π (or a higher multiple). Problem 14.4 will show that this phase shift occurs around the resonance frequency $\omega = 1/\sqrt{L_m C_m}$. This means that any noise initially in the circuit at that frequency will grow exponentially until it either clips or is intentionally limited. This mechanism is used to generate the clocks for almost all digital systems.

The great advantage of using a piezoelectric crystal rather than an ordinary inductor and capacitor comes in the performance of its effective components. Quartz (SiO_2) is the most commonly-used material, because it is literally as cheap as sand, and because its mechanical parameters can have a weak thermal dependence. The resonant mode used more frequently is a thickness shear, but flexural resonances and higher-order modes can also be excited, and it's possible to use a *Surface Acoustic Wave* (*SAW*) instead of these bulk acoustic waves [Kino, 1987]. For a quartz resonator, C_m is typically on the order of femtofarads and L_m is millihenrys, giving resonant frequencies on the order of megahertz, with overtones up to hundreds of megahertz. Capacitors and inductors in this range would be much more susceptible to parasitic coupling and thermal drift. Even worse, the Q of a conventional LC circuit is $\sim 10-100$. For a quartz resonator, it's $\sim 10^4-10^5$ because the mechanical damping due to *internal friction* is much smaller than the comparable electrical resistance. Since the Q is equal to $f/\delta f$, the inverse limits the relative uncertainty $\delta t/t$ in the time derived the resonator.

The dominant frequency variation in a quartz resonator comes from thermal drifts changing its stiffness. This can be corrected by measuring the temperature and using it to tune the resonator circuit in a *TCXO* (*Temperature Compensated Crystal Oscillator*), reducing the relative error to $\sim 10^6$. Even better, an *OCXO* (*Oven Compensated Crystal Oscillator*) fixes the temperature of the resonator, and can do that at the temperature where quartz is least sensitive to drift, reducing the short-term relative error to $\sim 10^{-8}$ [Walls & Vig, 1995].

Measuring time to a part in 10^8 may sound impressive, and it is, but it's not hard to need more. An error of 1 ns will be made in $\sim 10^{-9}\ \text{s} \times 10^8 = 0.1$ s. Since electromagnetic radiation travels 1 ft/ns, this means that if a quartz oscillator is used to determine the arrival time of an RF signal, it will be off by the equivalent of 10 feet after running for 1

second, a difference of some concern if you're trying to use it to land an airplane. And as important as the *precision* (variance) is the *accuracy* (bias). The resonant frequency of a quartz oscillator is determined by its mechanical properties. Even if these are sufficiently stable, if the resonator wasn't cut to exactly the right length or if its stiffness changes from aging then the airplane will predictably land in the middle of a field.

Both of these problems are solved by recognizing that macroscopic objects can differ, but the microscopic properties of all atoms are identical. Quantum mechanically there is no way to distinguish between two atoms, so clocks based on atomic resonators will keep the same time. This is an old idea [Kusch, 1949] that has both required and enabled a great deal of new technology [Major, 1998].

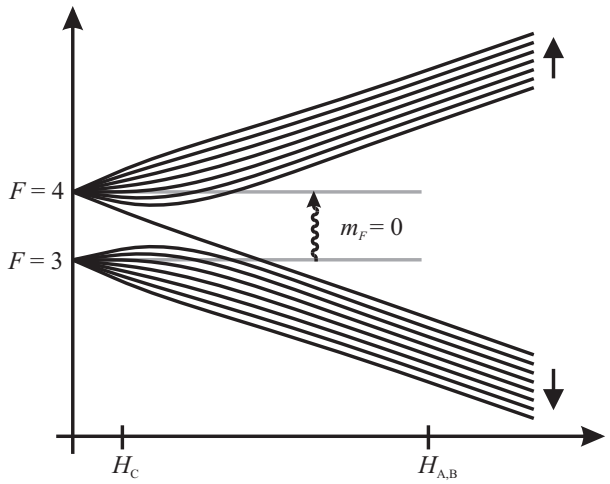

Figure 14.5. Cesium energy levels.

Cesium has one stable isotope, ^{133}Cs, with a nuclear spin of $I = 7/2$. There is a single outer electron, which in its ground state is in an s orbital with angular momentum $L = 0$. Therefore, since the electron spin is $S = 1/2$, its total angular momentum $J = L + S$ can be $\pm 1/2$. If the electron is parallel to the nucleus, the angular momentum of them together is $F = I + J = 4$, and if it is antiparallel $F = 3$. These energies will be split because of dipole–dipole coupling between the electron and the nucleus. This is called *fine structure*, because the scale is smaller than transitions between outer electron levels.

Chapter 16 will discuss the addition of quantum angular momentum, and the allowed spin states. The component m aligned with a magnetic field is quantized in integer steps, so that for $F = 3, m = -3, -2, \ldots, 2, 3$. The energies of these states are split due to the dipolar coupling to the field, revealing *hyperfine structure* as the field is increased. In the limit of a strong magnetic field the relative orientation of the electron and nuclear spins no longer matters, and the energy depends only on the alignment with the field. This is shown in Figure 14.5.

Now consider the *atomic clock* shown in Figure 14.6. Cesium atoms emerge from an oven into a vacuum chamber, and then pass through a strong magnetic field with a gradient. It's energetically favorable for one group of states to be in a weaker field, and the other in a stronger field, so they split into two beams. An aperture selects just

one of these. The cesium atoms then enter into a region with a uniform magnetic field, carefully screened from external fields. Microwaves are applied with a frequency tuned to the $F = 3 \rightarrow 4$ transition between $m_F = 0$ levels, which to first order are independent of the magnetic field. The field used is just strong enough to split the hyperfine states, but not so strong as to start separating the multiplets.

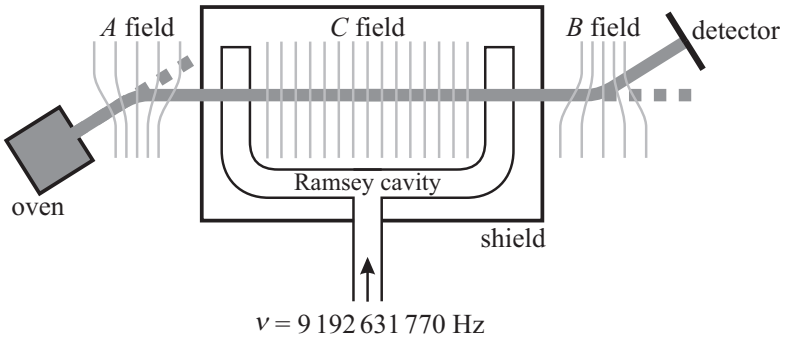

Figure 14.6. Cesium beam atomic clock.

Then the cesium beam passes through another strong gradient field. With no RF applied, the atoms once again are attracted in the direction of the stronger field, pulling them to a detector. But if the RF exactly matches the $F = 3 \rightarrow 4, m_F = 0$ transition frequency, atoms will emerge in the multiplet with the opposite orientation, being attracted to the weaker field and changing the flux reaching the detector. By modulating the RF, and feeding back the detector signal, its frequency can be locked onto the resonance. The frequency of this transition has now become one of the fundamental constants defining the SI system, $\nu = 9\,192\,631\,770$ Hz. The spectral linewidth is limited by the frequency–time uncertainty from passing through the field, which is improved by making the middle region as long as possible. A *Ramsey cavity* reduces the required homogeneity by applying the RF coherently at just the beginning and end of the interval [Ramsey, 1980].

Switching from quartz to a cesium beam reduces the relative uncertainty in the time to $\sim 10^{-12}$. By using lasers to perform the state selection, and to cool the atoms so that they can be dropped in a gravitational *fountain*, this can be extended to $\sim 10^{-15}$ [Gibble & Chu, 1993]. And this spectacular performance is as stable and repeatable as the quantum states of the atom, which as far as we can tell does not have a cosmological drift.

14.3.2 Time

Atoms might not drift, but time itself can. This shocking conclusion follows from the failure of the Michelson–Morley experiment in 1887 to observe a difference in the speed of light moving parallel and perpendicular to the Earth's orbit that would be caused by motion through a medium carrying electromagnetic waves. This, plus Lorentz's development of transformations between inertial frames that leave Maxwell's equations unchanged, led to the theory of *special relativity* [Einstein, 1916]. The lack of an electromagnetic ether also helped lead to the recognition that electromagnetic radiation is quantized in photons.

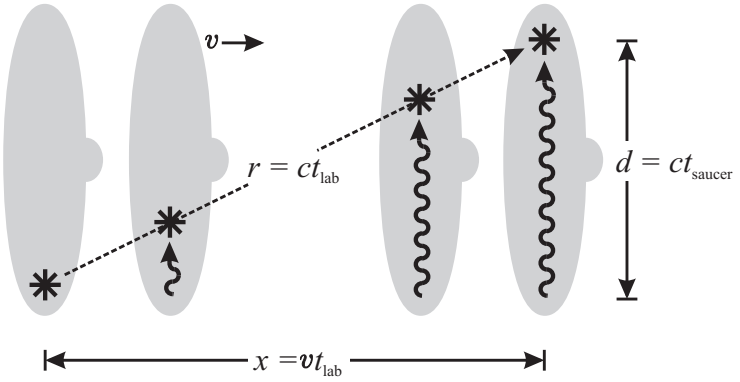

Figure 14.7. Time dilation.

Figure 14.7 shows why the experimental observation that the velocity of light is constant regardless of the relative motion of the emitter and detector implies that time must not be. A flying saucer is passing by with a velocity v. At $t = 0$ there is a flash of light, and both a stationary observer in the lab and a moving observer on the flying saucer synchronize their clocks. If the saucer has a diameter d, the flash will reach the far end when $d = ct_{\text{saucer}}$. At that instant the rocket will have traveled $x = vt_{\text{lab}}$, and in the lab frame the light will have traveled a distance $r = ct_{\text{lab}}$. The times in the two frames can be related by reconciling this geometry:

$$\begin{aligned} r^2 &= x^2 + d^2 \\ c^2 t_{\text{lab}}^2 &= v^2 t_{\text{lab}}^2 + c^2 t_{\text{saucer}}^2 \\ t_{\text{lab}} &= \frac{t_{\text{saucer}}}{\sqrt{1 - v^2/c^2}} \\ &\equiv \gamma t_{\text{rocket}} \quad . \end{aligned} \tag{14.55}$$

More time appears to pass in the lab than on the saucer, with time in the moving frame stopping in the limit $v \to c$ (!). This *time dilation* must be the most dramatic application of Pythagoras' Theorem.

Scaling time in turn implies that momentum is also scaled between moving frames,

$$p = mv = m\frac{dx}{dt} \;\rightarrow\; m\frac{dx}{dt}\gamma = mv\gamma \quad . \tag{14.56}$$

Since energy is the integral of force times displacement, and force is the rate of change of the momentum in a frame, the energy after accelerating from 0 to v is

$$\begin{aligned} E &= \int_0^v F\, dx \\ &= \int_0^v \frac{dp}{dt}\, dx \\ &= \int_0^v \frac{dx}{dt}\, dp \\ &= \int_0^v v'\, dp \end{aligned}$$

$$
\begin{aligned}
&= \int_0^v v'\, d(mv'\gamma) \\
&= m\int_0^v v'\, d\left[\frac{v'}{\left(1 - v'^2/c^2\right)^{1/2}}\right] \\
&= m\int_0^v v'\left[\frac{1}{\left(1 - v'^2/c^2\right)^{1/2}} + \frac{v'^2/c^2}{\left(1 - v'^2/c^2\right)^{3/2}}\right] dv' \\
&= m\int_0^v \frac{v'}{\left(1 - v'^2/c^2\right)^{3/2}}\, dv' \\
&= \frac{mc^2}{\left(1 - v^2/c^2\right)^{1/2}} \\
&= mc^2\gamma \quad . \qquad (14.57)
\end{aligned}
$$

In the low-velocity limit this has the famous form

$$E = \frac{mc^2}{\left(1 - v^2/c^2\right)^{1/2}} \approx mc^2 + \frac{1}{2}mv^2 \quad . \qquad (14.58)$$

The appearance of a *rest mass* energy mc^2 associated with matter rather than motion had enormous implications for physics (and everything else).

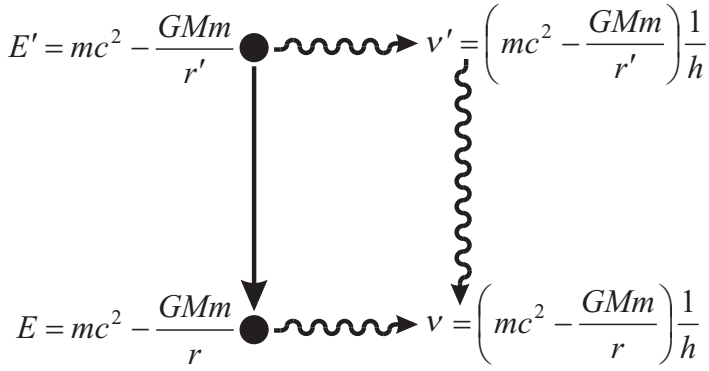

Figure 14.8. Gravitational red shift.

Now consider what happens when a mass m is moved in the gravitational field of a mass M from a radius r' to r, as shown in Figure 14.8. The rest mass energy doesn't change, but the gravitational potential energy does. From quantum mechanics we know that $E = h\nu$, so that in either position it's possible for all of the energy (rest plus potential) to be converted into a photon with frequency E/h. But then there's a problem, because if the photon instead of the mass travels from r' to r, the energies no longer match. By converting the photon back into mass, depending on the direction it travels it's possible to either run the cycle as a perpetual motion machine or cause the mass to vanish. Since that's an appealing but as far as we know entirely impossible outcome, the more plausible conclusion is that the frequency of light must depend on gravity. This is called the *gravitational red shift*.

In the last section we saw that electromagnetic oscillations define time, so the relative time at two radii must also be scaled by the ratio of the frequencies

$$t = \frac{1 - \dfrac{GM}{rc^2}}{1 - \dfrac{GM}{r'c^2}}\, t' \quad . \tag{14.59}$$

Time slows down as gravity increases, one of the most surprising predictions from *general relativity*, the extension of special relativity to include gravity [Einstein, 1905]. The seeds of quantum mechanics were lurking in the invariance of the speed of light in special relativity, and we obtained the red shift by combining quantum mechanics with special relativity, but to date gravity itself has defied a quantum explanation [Hawking, 1993].

The apparent passage of time depends on motion, and on gravity. While not familiar from our non-relativistic everyday experience, these effects are not only measurable by an atomic clock, they are essential corrections needed by practical electromagnetic ranging systems (Problem 14.6).

14.3.3 Position

The history of time is intimately tied to the history of navigation. The latitude of a ship at sea can easily be determined from the stars, but because of the Earth's rotation a reliable time reference is needed to find its longitude. A catastrophic shipwreck in 1707 led the British government to offer a large prize for an improved chronometer, which was eventually claimed by John Harrison in 1765 for a clever mechanical design good to better than 1 s/day, a relative error of 10^{-5} that is competitive with today's quartz clocks [Sobel, 1996].

British ships sailing from London set their chronometers by observing a red ball dropped on a pole above the Royal Observatory in Greenwich at 1 pm every day (chosen to follow noon astronomical observations). This is why balls are dropped to mark new years, and why *UTC* (*Coordinated Universal Time*), originally called *GMT* (*Greenwich Mean Time*), is still measured from the zero degree meridian that passes through the Observatory. While modern position measurement systems have improved on the means for clock distribution, they still rely on timing measurements made relative to a reference event at a known time and location.

Schemes for timing radiation scattered from a passive object include *RADAR* (*RAdio Detection And Ranging*) [Skolnik, 1990], *LIDAR* (*LIght Detection And Ranging*), and *SONAR* (*SOund Navigation And Ranging*). Acoustic ranging is the simplest to implement because of the slow propagation speeds: at 20 °C the speed of sound is 343 m/s in air, 1482 m/s in water, and 5960 m/s in steel. These vary with temperature and ambient conditions, requiring environmental corrections and limiting the accuracy of absolute measurements. The index of refraction for light is a weaker function of atmospheric conditions, and it can propagate much further, but optical ranging requires timing on much faster scales. A *time of flight* measurement determines the distance directly from the arrival delay

$$d = v\,\Delta t \;\Rightarrow\; \Delta t = \frac{d}{v} \quad . \tag{14.60}$$

This can be converted to a phase measurement by modulating the light with an amplitude envelope with a frequency ν, so that an observed modulation phase shift $\Delta\varphi$ is related to the distance by

$$d = \frac{\Delta\varphi}{2\pi}\frac{v}{\nu} \;\Rightarrow\; \Delta\varphi = \frac{2\pi\nu d}{v} \quad . \tag{14.61}$$

Now ν can be selected to bring $\Delta\varphi$ into a convenient range. This is how *laser rangefinders* work [Rüeger, 1990].

In all of these systems the transmitter and receiver share a clock so that the timing needs only be reliable over the propagation interval. In a *bistatic* configuration the transmitter is separated from the receiver, putting much more stringent demands on their synchronization. And if an active receiver seeks to directly determine its position from multiple transmitters, they must each have reliable independent time references. The development of atomic clocks that can fly in a satellite makes this possible globally in the *GPS* (*Global Positioning System*) [Bhaskar *et al*., 1996].

GPS uses the *NAVSTAR* (*NAVigation System with Timing And Ranging*) constellation of 24 satellites at an altitude of 20 200 km in six orbital planes at an inclination to the equator of 55°. Each satellite transmits a message containing its orbital parameters (which are frequently updated from tracking ground stations) and the time from onboard atomic clocks. Knowledge of the distance to one satellite locates the receiver on a sphere, two satellites constrain it to a curve, and three to a pair of points (one of which is usually unphysical). To eliminate the need for the receiver to have an independent atomic clock to determine the range, the signal from a fourth satellite is used to overdetermine the geometry and let the three-dimensional position be found using only relative arrival measurements that can be performed with a quartz oscillator.

The satellites transmit at two frequencies, 1575.42 MHz and 1227.6 MHz, to enable correction of ionospheric propagation delays. To improve both the timing resolution and the interference rejection a spread spectrum modulation is used. There are two codes. The first, *C/A* (*Coarse/Acquisition*), has a sequence of 1023 chips that repeats every millisecond. This is used for the *Standard Positioning Service* (*SPS*) available to anyone, and to transmit the acquisition information for the cryptographically-encoded *Precise Positioning Service* (*PPS*) that has a period of seven days and is restricted to the military.

The resolution of PPS is on the order of 10 m. The possible C/A resolution is about 40 m; this was degraded by the infamous Selective Availability (SA) program to 100 m to limit the strategic use of GPS. These intentional random errors were eliminated in *DGPS* (*Differential GPS*) by using the signal from a ground station with a known location to deduce the correction. With averaging, GPS is used for sub-centimeter measurements of geolotical motion [Herring, 1999].

Problem 14.6 looks at the importance of relativistic corrections to the nanosecond timing of the GPS atomic clocks. Relativity can also be applied directly to measure rotation through the *Sagnac effect*. It will take light a time

$$\tau = \frac{2\pi r}{c} \tag{14.62}$$

to be guided by mirrors or a fiber around a ring of radius r. If the ring is rotating at a

rate Ω, the tangential velocity is

$$\Omega\left(\frac{\text{rad}}{\text{s}}\right) \times \frac{1 \text{ cycle}}{2\pi \text{ rad}} \times \frac{2\pi r}{1 \text{ cycle}} = \Omega r \quad . \tag{14.63}$$

The speed of light is the same in the ring frame and in the laboratory frame, but the distance traveled is not. During the time τ the perimeter of the ring will have advanced by a distance $\Omega r\tau$. If the light is traveling in the direction of rotation this distance is added to its path, and if it is traveling in the opposite direction it is subtracted. The difference between the two paths is

$$\Delta l = 2\tau\Omega r = \frac{4\pi\Omega r^2}{c} \quad . \tag{14.64}$$

Beams sent in both directions and then recombined will generate interference fringes from the path difference. This provides a way to measure Ω that is robust because there are no moving parts, and has an enormous dynamic range because of the periodicity of the fringe pattern. The sensitivity can be increased by sending the light around many times, either through multiple fiber optic turns in a *fiber-optic gyroscope*, or by using the ring as the cavity of a laser in a *ring laser gyro* [Chow *et al*., 1985].

14.4 SELECTED REFERENCES

[Fraden, 1993] Fraden, Jacob. (1993). *AIP Handbook of Modern Sensors: Physics, Designs and Applications*. New York: American Institute of Physics.

$\sim$ 500 pages $\times$ 1 sensor/page.

[Tinkham, 1995] Tinkham, Michael. (1995). *Introduction to Superconductivity*. 2nd edn. New York: McGraw-Hill.

Superconductivity, with a strong emphasis on the phenomenology rather than the formal theory.

[Yourgrau *et al*., 1982] Yourgrau, Wolfgang, van der Merwe, Alwyn, & Raw, Gough. (1982). *Treatise on Irreversible and Statistical Thermophysics: an Introduction to Nonclassical Thermodynamics*. New York: Dover.

Werner Heisenberg "... likes this book very much indeed", and so do I.

[Major, 1998] Major, Fouad G. (1998). *The Quantum Beat: The Physical Principles of Atomic Clocks*. New York: Springer.

All of the physics behind, within, and beyond atomic clocks.

[Taylor & Wheeler, 1992] Taylor, Edwin F., & Wheeler, John Archibald. (1992). *Spacetime Physics: Introduction to Special Relativity*. 2nd edn. New York: W.H. Freeman.

A marvelous guide to special relativity.

[Misner *et al*., 1973] Misner, C.W., Wheeler, J.A., & Thorne, K.S. (1973). *Gravitation*. New York: W.H. Freeman & Co.

A marvelous guide to general relativity.

14.5 Problems

(14.1) Evaluate a Taylor expansion of equation (14.6) around $V = 0$.

(14.2) Problem 6.5 showed that for a Kibble balance the current I measured in the dynamic phase and the voltage V measured in the static phase are related to the mass m, gravitational constant g, and velocity v by $IV = mgv$. Using the inverse AC Josephson effect (equation 14.25) to determine the voltage, and the quantum Hall effect (equation 13.41) along with the inverse AC Josephson effect to determine the current, relate the measurement to fundamental constant(s).

(14.3) If a SQUID with an area of $A = 1$ cm^2 can detect 1 flux quantum, how far away can it sense the field from a wire carrying 1 A?

(14.4) Typical parameters for a quartz resonator are $C_e = 5$ pF, $C_m = 20$ fF, $L_m = 3$ mH, $R_m = 6\ \Omega$. Plot, and explain, the dependence of the reactance (imaginary part of the impedance), resistance (real part), and the phase angle of the impedance on the frequency.

(14.5) If a ship traveling on the equator uses one of John Harrison's chronometers to navigate, what is the error in its position after one month? What if it uses a cesium beam atomic clock?

(14.6) GPS satellites orbit at an altitude of 20 180 km.

(*a*) How fast do they travel?

(*b*) What is their orbital period?

(*c*) Estimate the special-relativistic correction over one orbit between a clock on a GPS satellite and one on the Earth. Which clock goes slower?

(*d*) What is the general-relativistic correction over one orbit? Which clock goes slower?